

Observing compact quark matter droplets in relativistic nuclear collisions

K. Paech^a, J. Brachmann^a, M. A. Lisa^b, A. Dumitru^c, H. Stöcker^a, W. Greiner^a

^a Institut für Theoretische Physik, Universität Frankfurt a.M., Postfach 111932,
D-60054 Frankfurt am Main, Germany

^b Department of Physics, The Ohio State University, 174 W. 18th Avenue,
Columbus, Ohio 43210, USA

^c Department of Physics, Columbia University,
538 W. 120th Street, New York, NY 10027, USA

Oct. 2000

Abstract

Compactness is introduced as a new method to search for the onset of the quark matter transition in relativistic heavy ion collisions. That transition supposedly leads to stronger compression and higher compactness of the source in coordinate space. That effect could be observed via pion interferometry. We propose to measure the compactness of the source in the appropriate principal axis frame of the compactness tensor in coordinate space.

A variety of signatures for the observation of the quark matter transition in relativistic heavy ion collisions have been proposed, see e.g. [1] and references therein. Nowadays it is widely believed that irregularities due to such a new state of matter should be seen most clearly in excitation functions, i.e. in the bombarding energy dependence, or possibly also in the impact parameter or mass-number dependence of various observables.

However, in spite of circumstantial evidence for such a novel state of matter [2], undisputable “irregularities” in such experimental excitation functions have not been reported to date. Most probably a convincing argument that quark matter has indeed been found requires several independent measurements of distinct observables pointing to the same conclusion - namely the onset of deconfinement at a particular bombarding energy, impact parameter and system size.

In the present paper we introduce a new observable for the onset of the phase transition. It relies on the measurement of the compactness of the source, which is related to the pressure and density of the system in the compression and expansion stage of the nucleus-nucleus collision. Observables related to the pressure do not only reflect the transient high density but rather relate to the *order parameter* (field), specifying in which thermodynamical *state* [3] the excited matter was created. The compactness can be identified via interferometry: The illumination of the baryon source by the pion radiation is subject to experimental scrutiny via pion interferometry measurements [4].

To illustrate the basic idea, let us first discuss compression shocks in heavy-ion collisions employing the Rankine Hugoniot Taub shock adiabat (RHTA) solution [5, 6] of relativistic hydrodynamics,

$$W^2 - W_0^2 + P \left(\frac{W}{\rho} - \frac{W_0}{\rho_0} \right) = 0 \quad . \quad (1)$$

It relates the energy per baryon in the local rest frame of the compressed matter, W , to its baryon density ρ and pressure P . W_0 and ρ_0 are the energy (=923 MeV) and density (=0.16 fm⁻³) in the ground state, and the compression factor is ρ/ρ_0 .

Solving for P we obtain

$$P = W\rho_0 \frac{\gamma_{\text{cm}} - 1/\gamma_{\text{cm}}}{1 - \gamma_{\text{cm}}\rho_0/\rho} \quad . \quad (2)$$

Simply speaking, the onset of the transition to quark matter at a given incident energy $E_{\text{lab}}^{\text{kin}} = 2(\gamma_{\text{cm}}^2 - 1)W_0$ lets the pressure increase less rapidly with W and/or ρ , and consequently higher compression ρ/ρ_0 can be achieved than for the case without transition. Now, as $\rho V \simeq \pi R_A^2 L \rho$ must equal $2A$ by virtue of baryon number conservation, the longitudinal thickness L of the compressed matter is proportional to $1/\rho$. Thus, a transition to quark matter leads to a more compact system, just as compact stars with a quark matter core are

more compact than pure neutron stars [7]. Of course, in heavy-ion collisions that expectation is based on the behavior of relativistic compression shocks rather than hydrostatic and gravitational equilibrium.

To investigate quantitatively the experimental observable, we perform 3-dimensional (1-fluid) calculations of relativistic hydrodynamics for the compression as well as for the subsequent expansion stage of the reaction. That is, we solve numerically the continuity equations for the energy-momentum tensor, $\partial_\mu T^{\mu\nu} = 0$, and the net baryon current, $\partial_\mu N_B^\mu = 0$. Detailed discussions of (3+1)-d numerical solutions for hydrodynamical compression and expansion can be found e.g. in [8]. We shall employ two different equations of state (EoS) $P(W, \rho)$: i) a relativistic mean field (RMF) hadron fluid [9] corresponding to baryons and antibaryons interacting via exchange of massive scalar and vector bosons, plus free thermal pions; the parameters of the lagrangian are fitted to the ground state of infinite nuclear matter, in particular the nuclear saturation density, the energy per nucleon, and the incompressibility. ii) the same EoS as in i) for the low-density phase, supplemented by the Bag Model equation of state with bag constant $B^{1/4} = 235$ MeV for the quark-gluon (QG) phase. The phase coexistence region corresponding to this first-order transition is constructed employing Gibbs' condition of phase equilibrium, $p_{\text{RMF}}(T, \mu_B) = p_{\text{QG}}(T, \mu_B)$, where T and μ_B denote the temperature and the baryon-chemical potential, respectively. For example, for $\rho = 0$ we find $T_C \approx 170$ MeV, while at $T = 0$ phase coexistence sets in at $\rho \approx 4.6\rho_0$. A more detailed discussion of these EoS can be found in [6].

As an example, we study the compactness in the reactions Au+Au at impact parameter $b = 3$ fm and energy $E_{\text{lab}}^{\text{kin}} = 8A$ GeV, where the transition to quark matter does occur (within the present model). We define the configuration space sphericity tensor, also called ‘‘compactness tensor’’ below, as the second moment of the net baryon current. On fixed time hypersurfaces we have

$$F_{ij}(t) = \int d^3x x_i x_j N_B^0(t, \vec{x}) \Theta(\rho(t, \vec{x}) - \rho_{\text{cut}}) \quad . \quad (3)$$

We apply an additional density cut $\rho > \rho_{\text{cut}}$ in the integral to discard spectator matter. In the future the cuts and the hypersurface will have to be adapted to the experimental conditions. However, that is not crucial for understanding the effect.

The three eigenvalues f_n are the solutions of the cubic equation $\det(F_{ij} - f\delta_{ij}) = 0$, and the eigenvectors \vec{e}_n follow from solving the linear system of equations $(F_{ij} - f_n\delta_{ij})e_n^j = 0$. Let \vec{e}_1, \vec{e}_2 be the eigenvectors defining the reaction plane, \vec{e}_1 corresponding to the bigger of the eigenvalues f_1 and f_2 . To simplify the discussion we shall assume that the matter distribution is symmetric with respect to the reaction plane.

We can now rotate the coordinate frame around \vec{e}_3 by an angle $\cos \Theta = \vec{e}_1 \cdot \vec{e}_z$, where \vec{e}_z

defines the longitudinal (beam-) direction in the lab frame. The rotated compactness tensor F^* can be written in terms of the eigenvalues f_n and orthogonal eigenvectors \vec{e}_n^* as

$$F^* = f_1 \vec{e}_1^* \otimes \vec{e}_1^* + f_2 \vec{e}_2^* \otimes \vec{e}_2^* + f_3 \vec{e}_3^* \otimes \vec{e}_3^* \quad . \quad (4)$$

In diagonal form, F^* specifies an ellipsoid in configuration space with principal axis along \vec{e}_n^* and radii $\sqrt{f_n}$. For example, cigar patterns, oriented along the z-axis, would correspond to $f_1 > f_2 = f_3$, $\vec{e}_1^* = \vec{e}_z$, $\vec{e}_2^* = \vec{e}_x$, $\vec{e}_3^* = \vec{e}_y$. The ‘‘compactness’’ can now be defined as the ratio of the in-plane radii, $\sqrt{f_2/f_1}$.

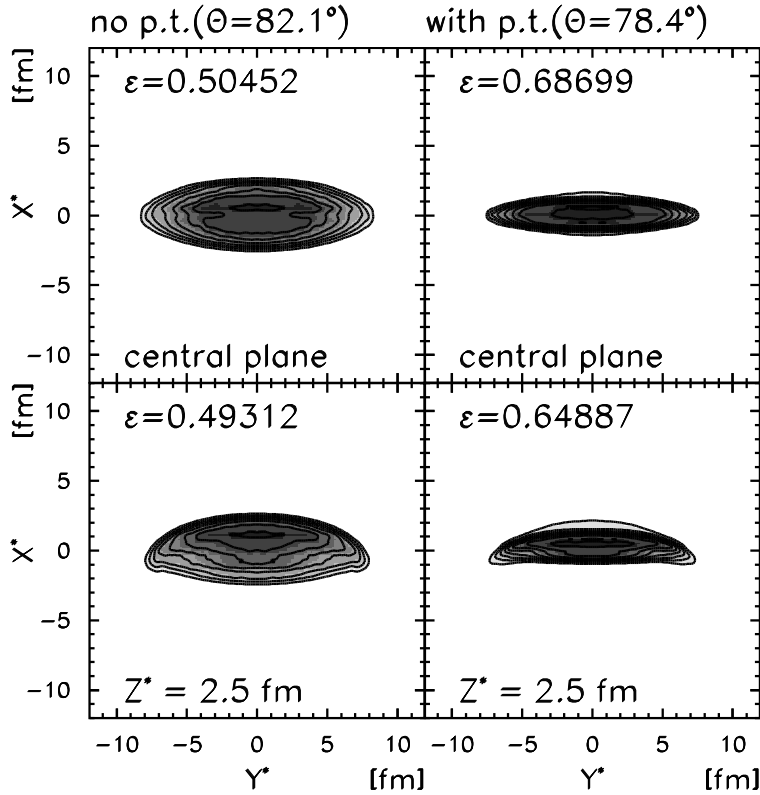


Figure 1: Contour plot of the time-like component of the net baryon four-current in planes transverse to the longitudinal axis \vec{e}_1^* of the compactness tensor (Au+Au collision at $E_{lab}^{kin} = 8$ AGeV, $b = 3$ fm). Left: Relativistic mean-field EoS without phase transition. Right: with phase transition to quark matter.

Fig. 1 shows typical density distributions in the transverse planes of the coordinate frame where F^* is diagonal, eq. (4). The polar angle relative to the lab frame as well as the eccentricity

$$\epsilon = \frac{f_3 - f_2}{f_3 + f_2} \quad (5)$$

are shown as well. As already indicated in the introduction, we find very different eigenvalues for the two equations of state, the one without and the other with a first order phase transition included. The calculation with transition to quark matter corresponds to higher compactness of the baryon distribution. Because the incompressibility $\partial p/\partial\rho$ or $\partial p/\partial(W\rho)$ is smaller in the presence of the coexistence phase, the compactness tensor is much flatter (nearly a factor of two !) in model ii) than in model i). Moreover, our (3+1)-dimensional expansion solutions show that the ratio of the in-plane radii $\sqrt{f_2/f_1}$ remains much smaller in the case with phase transition, cf. Fig. 2.

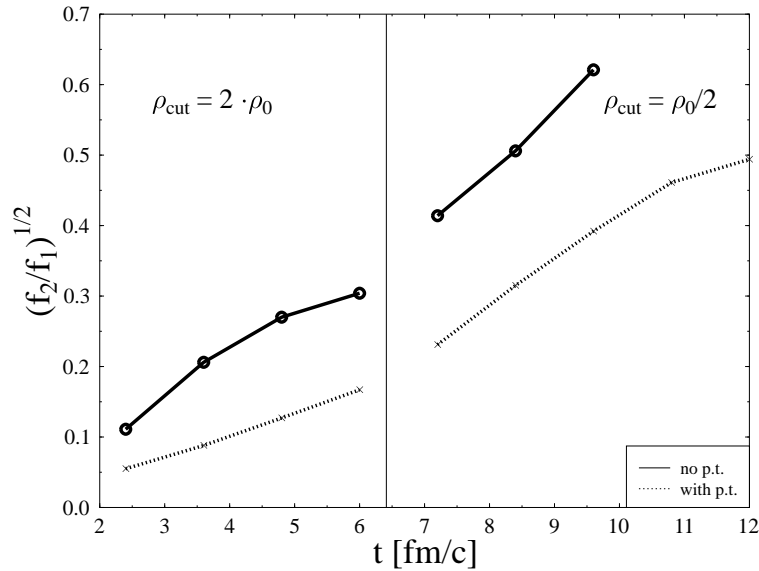


Figure 2: Ratio of the in-plane radii $\sqrt{f_2/f_1}$ as it evolves during the compression and expansion stages, for the relativistic mean-field EoS without phase transition and for the case with transition to quark matter (Au+Au, $E_{\text{lab}}^{\text{kin}} = 8$ AGeV, $b = 3$ fm).

This allows to measure directly the density increase in the high density stage of the reaction, if a phase transition occurs. Care must be taken that the investigated range of impact parameters constitutes a moderately small bin of centrality values. One should keep in mind that the compression factor is affected by the incompressibility evaluated on the RHTA (1), but *not* along a path of fixed specific entropy, because a large amount of entropy is being produced in the compression process.

The predicted change in compactness due to the reduced incompressibility associated with a first-order phase transition can be observed experimentally via the novel interferometry analysis developed recently by Lisa *et al.* [4]. The proposed method is quite robust and

incorporates other interesting information as the configuration space tilt angles [10], which complement the momentum-space flow angles. It avoids cuts in tilted ellipsoids, which are not analysed in the appropriate rotated frame, and were the eccentricity and the RMS-radii are much less distinct for models i) and ii).

Acknowledgements: This work is supported by BMBF, GSI, DFG, and Graduiertenkolleg “Theoretische und Experimentelle Schwerionenphysik”. A.D. acknowledges support from the DOE Research Grant, Contract No. De-FG-02-93ER-40764. We would like to thank Stefan Scherer, Sven Soff and Steffen Bass for stimulating discussions.

References

- [1] Proceedings of the 14th Intern. Conference on Ultrarelativistic Nucleus-Nucleus Collisions (Quark Matter 99), Torino, Italy, 10–15 May 1999, Nucl. Phys. **A661**, 1 (1999).
- [2] U. Heinz and M. Jacob, nucl-th/0002042.
- [3] T. D. Lee and G. C. Wick, Phys. Rev. **D9**, 2291 (1974).
- [4] M. A. Lisa, U. Heinz, and U. A. Wiedmann, nucl-th/0003022; M. A. Lisa, talk given at the Utah Winter Workshop RHIC 2000, <http://www.star.bnl.gov/~lisa/tilt/>, <http://www.nsl.msu.edu/~bauer/>.
- [5] H. G. Baumgardt *et al.*, Z. Phys. **A273**, 359 (1975); M. Gyulassy, K. A. Frankel and H. Stöcker, Phys. Lett. **B110**, 185 (1982).
- [6] D. H. Rischke, Y. Pürsün and J. A. Maruhn, Nucl. Phys. **A595**, 383 (1995).
- [7] N. K. Glendenning, “Compact stars: Nuclear physics, particle physics, and general relativity,” *New York, USA: Springer (1997) 390 p.*
- [8] D. H. Rischke, S. Bernard and J. A. Maruhn, Nucl. Phys. **A595**, 346 (1995); C. Nonaka, E. Honda and S. Muroya, hep-ph/0007187.
- [9] B. D. Serot and J. D. Walecka, Adv. Nucl. Phys. **16**, 1 (1986).
- [10] J. Brachmann, S. Soff, A. Dumitru, H. Stöcker, J. A. Maruhn, W. Greiner, L. V. Bravina and D. H. Rischke, Phys. Rev. **C61**, 024909 (2000).